Supporting Information

Growth chemistry and electrical performance of ultrathin alumina formed by area selective vapor phase infiltration

M. Snelgrove[a], C. McFeely[a], G. Hughes[a], C. Weiland[b], J.C. Woicik[b], K. Shiel[a], P.G. Mani González[c], C. Ornelas[d], Ó. Solís-Canto[d], K. Cherkaoui[e], P.K. Hurley[e], P. Yadav[f], M.A. Morris[f], E. McGlynn[a], R. O'Connor[a]

[a]*School of Physical Sciences, Dublin City University, Dublin 9, Ireland*

[b]*Materials Measurement Science Division, Material Measurement Laboratory, National Institute of Standards and Technology, Gaithersburg, Maryland 20899, USA*[*)]

[c]*Institute of Engineering and Technology, Department of Physics and Mathematics, Autonomous University of Ciudad Juárez, Cd. Juárez, Chihuahua 32310, Mexico*

[d]*Centro de Investigacion en Materiales Avanzados, Unidad Chihuahua, Chihuahua 31109, Mexico*

[e]*Tyndall National Institute, University College Cork, Lee Maltings, Prospect Row, Cork, Ireland*

[f]*AMBER Research Centre and School of Chemistry, Trinity College Dublin, Dublin 2, Ireland*

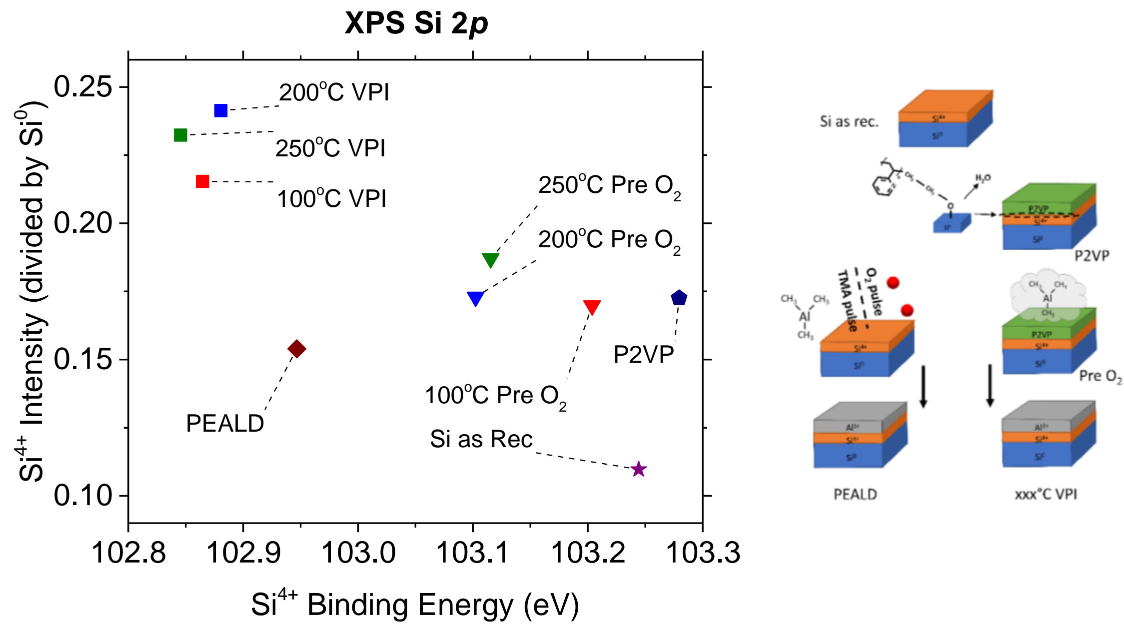

Figure S1: XPS intensity (using the Si 2p core level) of the Si^{4+} intensity versus it's corresponding binding energy position.

Prior to sample removal from vacuum, the Si/SiO_2/Alumina interface was monitored by XPS via acquisition of the Si 2*p*. The intensity of the silicon oxide is plotted against its corresponding binding energy position in Figure S1. The Si 2*p* was fitted with two components – one that represents the silicon bulk (Si^0) and the other representing Si^{4+}. The data was shifted so that the Si^0 peak occurs at 99.4 eV. For simplicity, silicon sub oxides were not included in the fit. The intensities of the Si^0 and Si^{4+} in the Si 2*p* XPS spectra were also used in accordance with literature for an approximation of the SiO_2 interlayer thickness.[1]

The PEALD process results in a slight increase of Si^{4+}, with the peak shifting to a lower binding energy. The growth in oxide may be attributed to the plasma dosing which results in the slight growth of the oxide, while the lower binding energy can be recognized as a consequence to aluminium silicates forming a thin interfacial layer between the Si and Al oxides.[2,3] The final thickness of this Si^{4+} interlayer was calculated as 0.6 nm.

The silicon undergoes more processing steps during the VPI process, with an initial growth of Si^{4+} observed in the P2VP film prior to VPI processing, attributed to the piranha acid treatment. A shift to lower binding energy is then observed during the VPI process prior to the plasma treatment (pre O_2) which suggests Si-O-Al bonding as in the PEALD film. Unlike in the PEALD process, no growth of the oxide was observed here however as no oxygen was present in this stage. However, significant growth and shifting to lower binding energy is observed for the polymer removal/metal oxidation step, with the VPI process containing significantly more of an Si oxide interlayer with potentially more Al silicates when compared to the PEALD approach. As is the case with the rest of the photoemission analysis, the different VPI temperatures behave consistently with respect to each other – all thicknesses of this interlayer were approximately 0.7 nm.

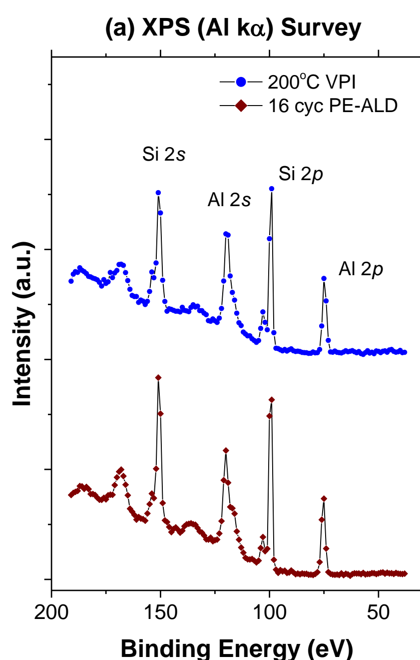

Figure S2: (a) XPS survey spectrum segment covering the Al 2p – Si 2s region. The PEALD process required only 16 ALD cycles for the film's Al 2p/Si 2p ratio to closely match that of the VPI alumina films.

The conclusions drawn from the ellipsometry, EDX and TEM results correlate with what was observed via XPS. The in-situ capabilities of the FlexAl – XPS system allows for the acquisition of ALD films of a specific thickness without the need to remove the sample from vacuum. By scanning a silicon substrate after a small number of PEALD cycles, it was found that a 16 cycle recipe produced alumina films with an Al 2*p*/Si 2*p* ratio that was almost identical to the films produced via a 100 °C, 200 °C and 250 °C VPI process, as observed in Figure S2. As XPS is a semiquantitative technique, the results from Figure S2 suggest that similar amounts of aluminium are present in the 16 cycle PEALD and VPI films. However, as the TEM showed, a further 19 cycles of TMA PEALD are required for the film to be of roughly equal thickness to the VPI films. This provides further confirmation that the VPI films are less dense with a higher degree of porosity

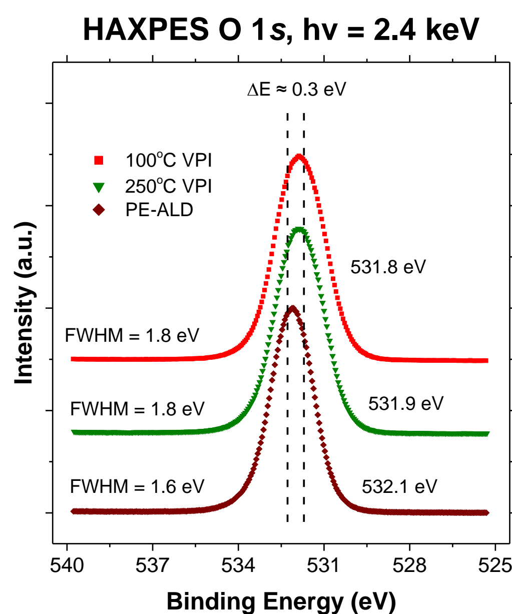

Figure S3: HAXPES spectra of the O 1s, with the binding energy positions of the spectra maxima labelled. The FWHM of the entire spectra is also displayed.

The O 1*s* spectra in Figure S3 consists of a combination of Si-O (from the SiO_2 interlayer) and Al-O bonds. SiO_2 bonds are expected to occur at approximately 533 eV, slightly higher than reported positions of Al_2O_3 which range from 530 eV to 532 eV.[4] The higher binding energy position of the peak maxima for the PEALD sample (532.1 eV) compared to the VPI samples (531.9 eV) is attributed to changes in the alumina film and the SiO_2 interface resulting from the different growth process. This has a secondary effect of decreasing the total full width half maximum (FWHM) of the spectra as the Si-O and Al-O components overlap more.

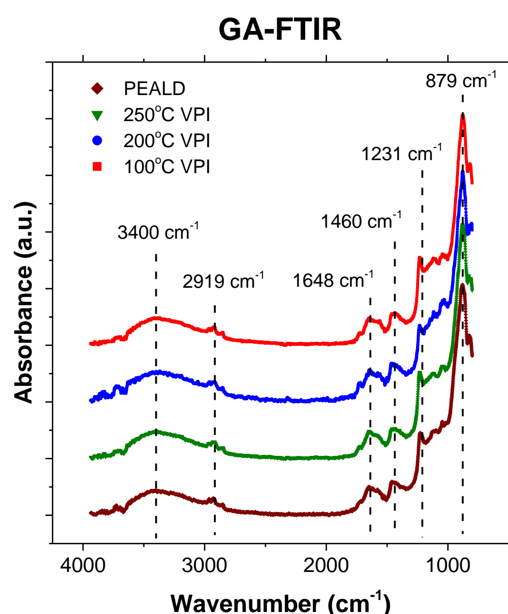

Figure S4: GA-FTIR spectra comparing VPI and PEALD made alumina films.

Grazing angle, attenuated total reflection Fourier transform infrared spectroscopy (GA-FTIR) was performed using a Nicolet iS50 FTIR Spectrometer with a Harrick VariGATR attachment. Absorbance spectra of the alumina films in Figure S4 exhibit almost identical spectral characteristics, with each sample containing significant amounts of OH in the film. The notable shoulder at approximately 3400 cm^{-1} is well known to represent OH stretching.[5] The peak at 1648 cm^{-1} is attributed to corresponding H_2O bending,[6,7] while the peak at 1460 cm^{-1} is potentially associated to Al-O-H stretching.[6,8] Adventitious carbon growth due to sample exposure to atmosphere are linked to the absorption bands at 879 cm^{-1} and 2919 cm^{-1}, which are associated with C-H bending and stretching respectively[9]. The peak at 1231 cm^{-1} is linked with C-O stretching.[10]

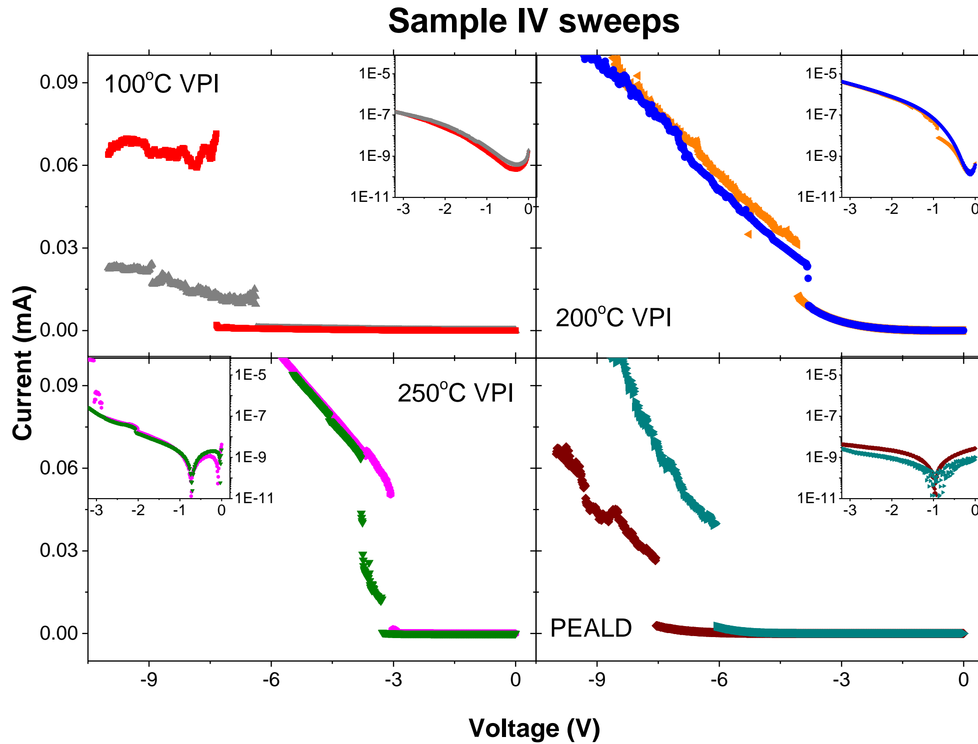

Figure S5: Sample IV sweeps for the 4 types of alumina samples analysed. Sweeps from 2 sites for each sample are shown. A sudden increase in current is determined as point of breakdown.

Sample IV sweeps are shown in figure S5. This measurement was repeated multiple times, with the average breakdown voltage recorded as –5.5 V, -3.9 V, -3.7 V and -7.2 V for the 100 °C VPI, 200 VPI °C, 250 °C VPI and PEALD films. These values were converted to breakdown field and underwent Weibull statistics to yield the distributions displayed in figure 2 of the main file for a more accurate assessment of the breakdown behaviour.

References

[1] D.S. Jensen, S.S. Kanyal, N. Madaan, M.A. Vail, A.E. Dadson, M.H. Engelhard, M.R. Linford, Silicon (100)/SiO 2 by XPS, Surf. Sci. Spectra. 20 (2013) 36–42. https://doi.org/10.1116/11.20121101.

[2] G.P. Gakis, C. Vahlas, H. Vergnes, S. Dourdain, Y. Tison, H. Martinez, J. Bour, D. Ruch, A.G. Boudouvis, B. Caussat, E. Scheid, Investigation of the initial deposition steps and the interfacial layer of Atomic Layer Deposited (ALD) Al2O3 on Si, Appl. Surf. Sci. 492 (2019) 245–254. https://doi.org/10.1016/j.apsusc.2019.06.215.

[3] O. Renault, L.G. Gosset, D. Rouchon, A. Ermolieff, Angle-resolved x-ray photoelectron spectroscopy of ultrathin Al2O3 films grown by atomic layer deposition, J. Vac. Sci. Technol. A. 20 (2002) 1867. https://doi.org/10.1116/1.1507330.

[4] J.F. Moulder, W.F. Stickle, P.E. Sobol, K.D. Bomben, Handbook of X-ray Photoelectron Spectroscopy, Perkin-Elmer Corporation, Eden Prairie, 1992.

[5] H.A. Al-Abadleh, V.H. Grassian, FT-IR study of water adsorption on aluminum oxide surfaces, Langmuir. 19 (2003) 341–347. https://doi.org/10.1021/la026208a.

[6] R.R. Toledo, V.R. Santoyo, D.M. Sánchez, M.M. Rosales, Effect of aluminum precursor on physicochemical properties of Al2O3 by hydrolysis/precipitation method, Nov. Sci. 10 (2018) 83–99. https://doi.org/10.21640/ns.v10i20.1217.

[7] J. Soria, J. Sanz, I. Sobrados, J.M. Coronado, A.J. Maira, M.D. Hernández-Alonso, F. Fresno, FTIR and NMR study of the adsorbed water on nanocrystalline anatase, J. Phys. Chem. C. 111 (2007) 10590–10596. https://doi.org/10.1021/jp071440g.

[8] A. Boumaza, L. Favaro, J. Lédion, G. Sattonnay, J.B. Brubach, P. Berthet, A.M. Huntz, P. Roy, R. Tétot, Transition alumina phases induced by heat treatment of boehmite: An X-ray diffraction and infrared spectroscopy study, J. Solid State Chem. 182 (2009) 1171–1176. https://doi.org/10.1016/J.JSSC.2009.02.006.

[9] B.H. Stuard, Infrared Spectroscopy: Fundamentals and Applications, John Wiley & Sons, Chichester, 2004.

[10] V. Tucureanu, A. Matei, I. Mihalache, M. Danila, M. Popescu, B. Bita, Synthesis and characterization of YAG:Ce,Gd and YAG:Ce,Gd/PMMA nanocomposites for optoelectronic applications, J. Mater. Sci. 50 (2015) 1883–1890. https://doi.org/10.1007/s10853-014-8751-9.